EXPERIMENTAL STUDY ON ACCUMULATION OF HELIUM RELEASED INTO A SEMI-CONFINED ENCLOSURE WITHOUT VENTILATION

Liang, Z., McKenna, A., Clouthier, T., David, R.
Canadian Nuclear Laboratories, Chalk River, Ontario, Canada
***Corresponding author*: zhe.liang@cnl.ca**

ABSTRACT

This paper presents a series of experiments performed at the Canadian Nuclear Laboratories to examine the dispersion behaviour of hydrogen in a semi-confined empty enclosure without ventilation. The purpose was to gain a better understanding of the effectiveness of natural or forced ventilation on potential hydrogen accumulation because of a leak. Although various hydrogen dispersion studies have been reported in the literature, gaps still exist in predictive methods for hydrogen hazard analysis. The tests reported in this paper were performed in a 16.6 m^3 polycarbonate enclosure. Helium, which was used as a simulant for hydrogen, was injected near the centre of the floor with a flow rate ranging from 2 to 50 SLPM through an upward-facing nozzle (25 mm in diameter), resulting in an injection Richardson number ranging between 0.3 and 134. When the flow rate was greater than 5 SLPM (Ri <100), the vertical helium profile always consisted of a homogenous layer at the ceiling overlaying a stratified layer. The difference in helium concentration between the top and bottom of the enclosure became larger with higher flow rates. In a long-term transient, a steady helium distribution was always reached with a uniform upper layer above a height of 1 m. The steady vertical helium distributions normalized by their volume-averaged concentrations were approximately self-similar for different injection rates. The measurements in this study were compared with results from analytical modelling and were found to be in good agreement when flow rates were greater than 5 SLPM.

1.0 INTRODUCTION

Hydrogen energy-based vehicles or power generators are foreseen to come into widespread use in the near future. Hydrogen safety information is of major importance to support the successful public acceptance of hydrogen as an energy carrier. One of the most important issues in terms of safety is the use of such systems in confined or semi-confined areas, such as private garages, underground parking, and long tunnels, due to potential accumulation of the flammable gas. Hydrogen dispersion in an enclosure is important for the assessment of potential combustion and development of mitigation measures. Various analytical [1]–[3] and experimental [4]–[8] studies have been reported in the literature.

Hydrogen mixing behaviour has also been extensively studied by the nuclear industry over the past three decades. At the Canadian Nuclear Laboratories (CNL), the Large-Scale Containment Facility (LSCF) was designed and constructed to investigate hydrogen–air–steam mixing behaviour using helium as a simulant, under high temperature and high humidity conditions analogous to what could exist in containment during various phases of a nuclear accident. Results from those experiments formed part of a database that has been used for the validation of GOTHIC [9] [10], a general purpose thermal-hydraulics code used by the nuclear community for safety analysis of containment thermal-hydraulics and of hydrogen transport and mixing behaviour following an accident.

The distribution of a buoyant gas in an enclosure depends on the release rate, momentum and buoyancy fluxes, volume of the enclosure, position of the source, and ventilation conditions of the enclosure [3]. For a low-momentum release, Baines & Turner [1] and Worster & Huppert [2] showed that a stratified layer can form and move downwards from the ceiling, whereas for a highly energetic jet, the concentration can be uniformly distributed in the enclosure [5]. Between these two situations, Bolster

and Linden [3] demonstrated that a vertical profile with an upper well-mixed layer followed by a stratified layer moving downwards can develop under certain release conditions. Baines & Turner [1] developed an asymptotic solution for the final state of the stratified layer during continuous release from small sources of turbulent buoyant plume into a sealed enclosure. Worster & Huppert [2] further developed a time-dependent density profile during downward movement of the stratified layer front based on Baines & Turner's theory. Bolster and Linden [3] also derived a simple model that takes into account the existence of an upper well-mixed layer above the stratified layers.

To have a better understanding of the dispersion mechanisms and to improve the predictive methods for hydrogen risk assessment within confined or semi-confined volumes at CNL, a series of experiments was performed to examine the helium dispersion behaviour under various release conditions and geometric configurations, simulating various kinds of leaks inside a confined or semi-confined enclosure. The focus of the paper was to identify dispersion regimes that may be encountered during the release of a buoyant gas in an empty enclosure with or without natural ventilation and wind as a function of release rates. The effect of forced ventilation, shape of the ceiling, and presence of obstructions will be examined in the future.

This paper presents results from a series of experiments performed in the semi-confined enclosure without ventilation. The experimental conditions used were similar to those of Cariteau et al. [4] and Cariteau & Tkaschenko [5], who performed tests in a 1 m^3 and 41.3 m^3 enclosure, respectively. The measurements were compared with predictions using both Baines & Turner's and Worster & Huppert's models [4] [5]. The experimental data will used for validation of our CFD codes for safety analysis.

2.0 EXPERIMENTAL METHODS

2.1 Facility

CNL's LSCF has a thick-walled concrete room with a total volume of approximately 1350 m^3. The enclosure is located inside the LSCF. A schematic of the enclosure is shown in Fig. 1. It had a total volume of approximately 16.6 m^3 (2.45 m high, 2.6 m long, and 2.6 m wide), and was constructed from engineered extruded aluminium beams and polycarbonate sheets. The polycarbonate sheets on the side walls had rubber seals along the seams. The sheets on the ceiling and floor were directly supported by horizontal beams. Silicone sealant was applied to the edges of the ceiling surface to eliminate leakage. There was an entry door (2 m tall and 0.75 m wide) on the left-side wall with rubber seals along the seams.

The enclosure had a straight pipe (25 mm or 1 in diameter) vertically placed inside the enclosure close to the front wall with three outlets at heights of 0.06, 1.0, and 2 m. The bottom opening was connected with the external helium supply. For the current tests, the middle and top outlets were capped, and the bottom outlet was extended to the bottom centre of the enclosure with a nozzle exit located approximately 10 cm (4 in) above the floor, pointing upwards. The nozzle had an internal diameter of 25 mm (1 in).

Two experimental setups were examined. In Configuration 1, silicone sealant was not applied to the edges of the floor surface, so distributed leaks were expected along the edges of the floor. In Configuration 2, the edges of the floor surface were sealed with silicone sealant and a 5 cm (2 in) circular opening was drilled in the floor surface (~1 m from the entrance door and ~20 cm from the side wall opposite the injection). Air entrainment was expected to be introduced primarily from the opening. Configuration 1 is referred to as "no seal" and Configuration 2 is referred to as "seal + hole" in this paper.

2.2 Measurements

The measurements consisted of helium flow rate, helium concentration, gas temperature, relative humidity (RH) and flow velocity through the opening. Each measurement is described below.

To maintain a constant flow rate during the test, the helium injection was regulated by a flow controller (Brooks 5851E). The controller had a maximum flow range up to 100 SLPM (standard litre per minute) and its accuracy was within ±0.5% of the full scale.

The helium concentration was measured by the XEN-5320-CAN bus system [11]. To monitor the helium spatial distribution, fifteen XEN-5320 sensors were installed in the enclosure. For both test configurations, fourteen sensors were mounted along the back wall opposite the helium inlets with four at heights from 0.25 to 1 m (spacing of 0.25 m), four from 1.2 to 1.8 m (spacing of 0.2 m), and six from 1.9 to 2.5 m (spacing of 0.1 m). For Configuration 2, one sensor was located close to the opening. Helium distribution was expected to be uniform on the horizontal plane away from plume, so one sensor at each elevation was considered to be sufficient to capture the global behaviour. All the sensors were reset to zero in helium-free atmosphere and to full span in pure helium atmosphere before each test series. The function of each sensor was verified using standard gases (1, 3, 5, 10, 20, and 50% helium in air). The measurement accuracy was within ±2% (relative) for 3–20%[1] helium in air and within ±0.2% helium (absolute) for 1% helium in air under ambient conditions (1 atm, 20°C, and ~50% RH).

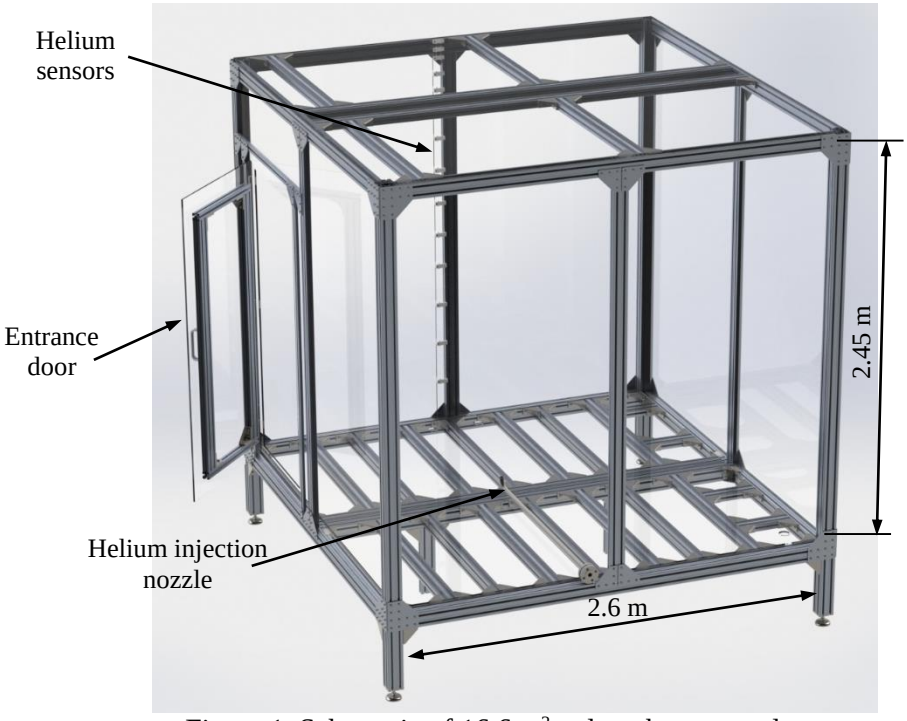

Figure 1. Schematic of 16.6 m^3 polycarbonate enclosure

To track potential thermal stratification, the gas temperature and RH inside the enclosure were measured on the gas sample side at heights of 0.5, 1.5, and 2.4 m, using calibrated K-type thermocouples and Vaisala HMP 235 RH probes. The uncertainty of the thermocouples was ±2°C to a 95% confidence level and the uncertainty of the RH probes was approximately ±3% RH. An in-house made bi-directional flow velocity probe was used for measuring the flow velocity through the opening for the Configuration 2 tests. Its measurement uncertainty was approximately ±0.1 m/s.

[1] The gas concentration is always expressed on a volume basis in this paper.

The flow injection rate, gas temperature, relative humidity, and flow velocity were recorded by a National Instruments PXI system at a sampling rate of 1 or 3 Hz. The helium concentrations were recorded using the XEN-5320-CAN bus communication software at the same sampling rate.

2.3 Test Conditions and Characteristic Parameters

A total of 12 dispersion tests were performed under ambient conditions (1 atm, ~20°C and ~50% RH), as summarised in Table 1. In each test, helium was continuously injected at a constant flow rate until a steady helium distribution profile was observed. The meaning of each characteristic parameter shown in Table 1 is explained below.

The measured flow rate, *Q*, is the average injection rate recorded during the entire transient. The nominal values (2, 5, 10, 20, 30, and 50 SLPM) are referred to in the paper. The flow velocity at the nozzle, U_0, varied from 0.08 to 1.63 m/s in these tests. The ratio of injection rate to enclosure volume, *Q/V*, denotes the theoretical average rate of helium fraction increase assuming no leakage of helium. The gas temperature, *T*, is an average of measurements from all three thermocouples during the entire transient. The value was approximately 19.5°C for all the tests. The average temperature difference, ΔT, between the top and the bottom thermocouples was less than 0.5°C.

Table 1. Summary of experimental conditions

Conf.	Measured Q		U_0 (m/s)	Q/V (h^{-1})	T (°C)	ΔT (°C)	R_i	B_0 (m^4/s^3)	L_m (m)	F (s^{-1})
	SLPM	m^3/s								
1- No seal	2.32	3.9E-05	0.08	0.39	19.5	0.3	131	3.31E-04	0.01	0.019
	5.29	8.8E-05	0.17	0.88	19.4	0.3	25.6	7.48E-04	0.03	0.024
	10.21	1.7E-04	0.34	1.70	19.5	0.3	6.8	1.45E-03	0.05	0.030
	20.09	3.4E-04	0.66	3.33	19.7	0.2	1.8	2.83E-03	0.10	0.038
	30.03	5.0E-04	0.99	4.97	19.6	0.1	0.8	4.23E-03	0.15	0.044
	49.49	8.3E-04	1.63	8.22	19.6	0.0	0.3	7.00E-03	0.25	0.051
2- Seal + hole	2.35	3.9E-05	0.08	0.39	19.5	0.3	131	3.31E-04	0.01	0.019
	5.31	8.8E-05	0.17	0.88	19.4	0.3	25.6	7.48E-04	0.03	0.024
	10.26	1.7E-04	0.34	1.70	19.5	0.3	6.8	1.45E-03	0.05	0.030
	20.11	3.4E-04	0.66	3.33	19.7	0.2	1.8	2.83E-03	0.10	0.038
	30.01	5.0E-04	0.99	4.97	19.6	0.1	0.8	4.23E-03	0.15	0.044
	49.63	8.3E-04	1.63	8.22	19.6	0.0	0.3	7.00E-03	0.25	0.051

The injection Richardson number, *Ri*, is defined as [4]:

$$Ri = \frac{\pi}{32}\frac{\rho_{air}-\rho_{He}}{\rho_{He}}\frac{gD^5}{Q^2}, \quad (1)$$

where ρ is the gas density, *D* is the nozzle diameter, *Q* is the helium injection rate, and *g* is the gravitational acceleration.

Depending on the order of magnitude of the Richardson number, the flow at the exit of the source may either be jet-like or plume-like. The exit flow is usually jet-like (momentum-dominant) in the case of $Ri << 1$, but the decrease in the exit velocity will lead to a transition to a plume-like (buoyancy-dominant) flow for a given distance from the source [5]. The order of magnitude of the Richardson number for the current tests varied between 10^{-1} and 10^2, suggesting that the flow would be dominated by buoyancy as soon as the fluid exited the injection nozzle.

The transition length, L_m, is defined as [12]:

$$L_m = 3\frac{(U_0 Q_0)^{3/4}}{{B_0}^{1/2}}, \quad (2)$$

where B_0 is the buoyancy flux, defined as [4] [5]:

$$B_0 = \frac{\rho_{air}-\rho_{He}}{\rho_{air}} gQ\ . \quad (3)$$

The transition length varied between 0.01 and 0.25 m for the current tests, meaning that the flow in the current tests was buoyancy-driven in most regions of the enclosure.

Time is non-dimensionalised by multiplying a normalization factor, F, defined as [4]:

$$t^* = F \times t \text{ and } F = H^{2/3}A^{-1}{B_0}^{1/3}, \quad (4)$$

where H is the height of the enclosure (= 2.45 m), and A is the horizontal cross-sectional area of the enclosure (= 6.76 m^2). The normalized time allows a better comparison of tests performed with different flow rates, gas types, and geometries.

3.0 RESULTS AND DISCUSSION

3.1 Leakage from Well-Mixed State

The leakage rate of the enclosure was determined using the tracer gas decay method presented by Gupta et al. [6]. Two leak tests were performed for each test configuration. In each test, helium was injected at 50 SLPM with a fan blowing across the injection nozzle to fully mix the helium in the enclosure. Helium injection stopped when the helium concentration reached 6.2% in the Configuration 1 test and 10.5% in the Configuration 2 test. The 5 cm (2 in) hole on the floor was blocked using aluminium tape after the helium injection stopped.

Fig. 2(a) shows the decay of the helium concentration normalized by its initial value for the Configuration 1 test. Time zero corresponds to the end of helium injection. The helium concentration at the floor starts decreasing immediately and the decay rate is also greater at lower elevations. These trends suggest that air either entered from the bottom of the enclosure or from the side, but moved to the bottom due to gravity, and the dilution started from the floor and gradually moved upwards.

Fig. 2(b) shows the logarithmic average helium concentration decay and leakage rate for both configurations. The average helium concentration $<He>$, in the total volume, was calculated by integration of the vertical profile shown in Fig. 2(a) with a trapezoidal rule assuming that the helium concentration is uniformly distributed horizontally. The normalized average helium concentration, $<He>/<He_0>$, is assumed to decay exponentially [6]:

$$\frac{<He>}{<He_0>} = \exp\left(-\frac{Q_L}{V}t\right) = \exp(-At), \quad (5)$$

where Q_L is the volume leakage rate and A (Q_L /V) denotes the air changes per hour (ACH) within the enclosure.

The slope of ln ($<He>/<He_0>$) gives an estimate of the ACH value, which is close to 0.3–0.4 shown in Fig. 2 (b), corresponding to a volumetric flow rate of 1.38–1.84×10^{-3} m^3/s (83–110 SLPM). The curves for the helium decay overlap for both configurations, indicating that the leakage rates are the same for both configurations. It suggests that the floor in Configuration 2 was not perfectly sealed.

As the temperature difference inside the enclosure is less than 0.5°C, the leakage was primarily driven by concentration gradients. It should be noted that the leakage rate depends on the initial helium volume fraction, and the value presented here should be considered in terms of order of magnitude.

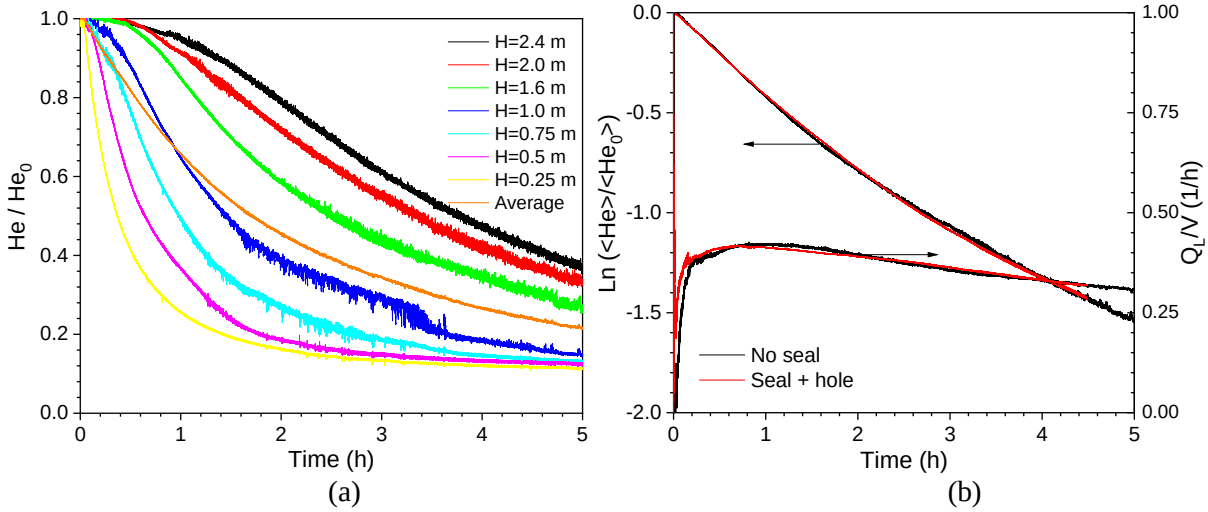

Figure 2. (a) Normalized helium concentration decay along height for Configuration 1, and (b) logarithmic normalized average helium concentration decay for both configurations

3.2 Leakage during Injection

The leakage during the helium injection is demonstrated in Fig. 3 by comparing the measured average helium concentration of the 12 tests shown in Table 1 with the theoretical value as a function of time, which is normalized by multiplying the theoretical average helium concentration increase rate, $Q/V \times 100$. Fig. 3 shows that the measurement is in good agreement with the theoretical value when the average concentration is less than 2–4%. This trend suggests that the leakage was insignificant when the injection time was shorter than 2–4 times of the ratio of V/Q. In the long term, the average helium concentration in the experiments is less than the theoretical value because of air exchange with the exterior. Fig. 3 also shows that the average helium concentrations for the two test configurations are identical at lower flow rates (2 and 5 SLPM), but the average concentration is slightly higher for Configuration 2 at higher flow rates. This means that the air entrainment is higher in Configuration 1, but the general behaviour is similar between the two configurations.

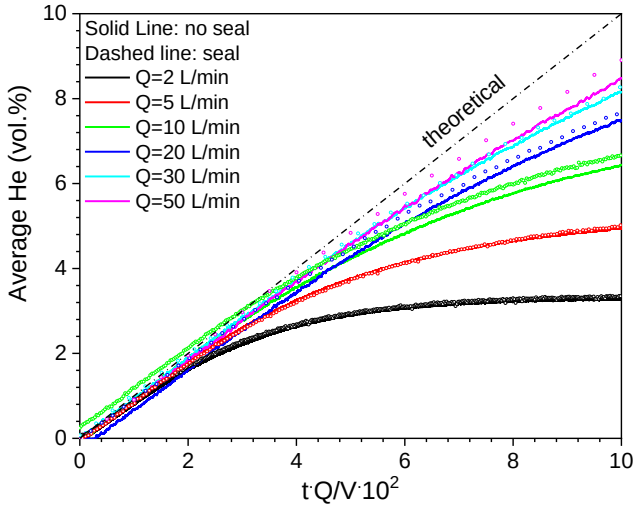

Figure 3. Normalized time transient of average helium concentration, <*He*>, during early release for both test configurations

3.3 Concentration Build-up

The normalized time transients of helium concentrations at various heights for the 2 and 30 SLPM tests with Configuration 1 are shown in Fig. 4. Time zero corresponds to the start of helium injection. As

show in Table 2, the physical time is 15 h at t* = 1000 for the 2 SLPM test and 5.1 h at t* = 800 for the 30 SLPM test.

In both tests, the helium concentration at all elevations increases linearly at the beginning, after an elevation-dependent delay, and then gradually reaches a steady state. At any given time, the helium concentration is always the highest at a higher elevation. It is well known that dispersion of a light gas in an enclosure will lead to an atmosphere of variable density. The density distribution in the enclosure during filling depends on the injection conditions [5]. When the flow is dominated by buoyancy, the density distribution is characterized by a stable vertical stratification. After the light gas reaches the ceiling, it starts to deflect horizontally to the side of the enclosure. A downward vertical flow then develops and occupies the entire horizontal section of the enclosure. A horizontal interface (known as the filling front) is formed between the upper part of the enclosure where the injected gas accumulates and the lower part where the density remains unchanged. In the upper layer, the mixture density decreases from the interface to the ceiling. The filling front moves downwards as the gas is injected.

For the two tests shown in Fig. 4, after the start of helium injection, the increase in the helium concentration at a height of 2.4 m is detected after ~92 s (t* = 1.70) for the 2 SLPM test and ~16 s (t* = 0.69) for the 30 SLPM test. This corresponds to the time when the helium plume arrives at the ceiling and the filling front starts moving downwards. The helium concentrations at lower elevations also start increasing gradually. In the short-term transient (Figs. 4a and 4c), the helium concentrations at all elevations increase linearly. At a given t*, the maximum helium concentration is much higher with a higher flow rate, and the stratification (concentration difference between a height of 2.4 and 0.25 m) is also larger.

In the long-term transient (Figs. 4b and 4d), the helium concentration at all elevations reaches a steady state, suggesting that the amount of helium injected is balanced with the amount of helium exchanged with the exterior. After t* = 500, the helium concentrations at all elevations approaches a steady state. The helium is almost fully mixed above a height of 1 m, but is highly stratified below 1 m. Cleaver et al. [13] proposed a criterion for a geometry without ventilation, where a well-mixed deep layer is formed when the distance between the release point and the ceiling, ΔH, is large in comparison to the characteristic dimension of the ceiling, namely $0.38\sqrt{A_c}$, where A_c is the ceiling surface area. In the present study, the distance between the release point and the ceiling is close to the height of the enclosure (2.45 m), which is much larger than the proposed criterion ($0.38 \times 6.76^{1/2} = 1.0$ m). The formation of a ceiling layer clearly also depends on the geometry dimensions, release conditions, ratio of momentum and buoyancy forces, and ventilation conditions.

The normalized time transients of helium concentration difference, ΔHe, between a height of 0.25 and 2.4 m and their values at t* = 500 (approaching steady state) are shown in Figs. 5a and 5b, respectively. As already demonstrated in Fig. 4, after the initial linear increase, the helium concentration reaches a steady value at all elevations in a long-term transient, and therefore a steady state for the concentration difference is also reached. The steady state is obtained much faster with a higher injection rate although the normalized time t* to reach steady state is close to 500 for all the tests. As seen in Fig. 5b, the steady state ΔHe increases quadratically as a function of the injection rate. At a given injection rate, ΔHe is higher with Configuration 1 than with Configuration 2. The reason is that the helium concentration at a height of 2.4 m is similar for the two configurations, but it is higher at a height of 0.25 m with Configuration 2 due to less air entrainment. For the tests performed by Cariteau et al. [4] in a "perfectly" sealed enclosure (leakage rate of 0.006 h^{-1}), the steady state is reached at t* = ~125[2] and the relationship between ΔHe and injection rate based upon Baines & Turner's solution [1] is in excellent agreement with their measurement. However, a much longer time is needed to reach a steady state in the present study due to a much higher leakage rate, and therefore the ΔHe value is much larger at a given flow rate.

[2] The t* value presented in Cariteau et al. [4] is twice as large; a mistake seems to have been made in their calculation.

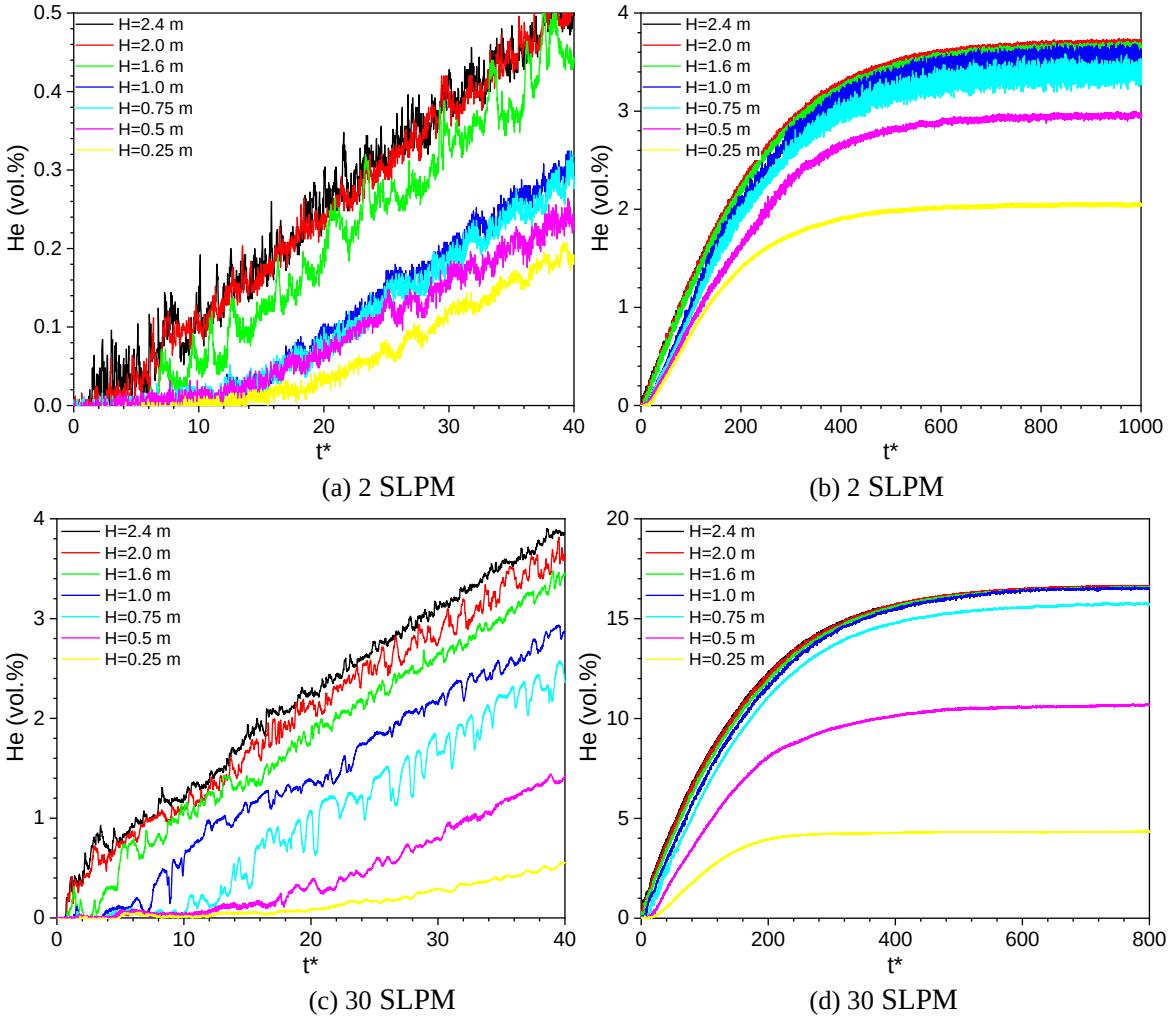

Figure 4. Short- and long-term time transients of helium concentrations along height for injection rates of 2 and 30 SLPM with floor not sealed

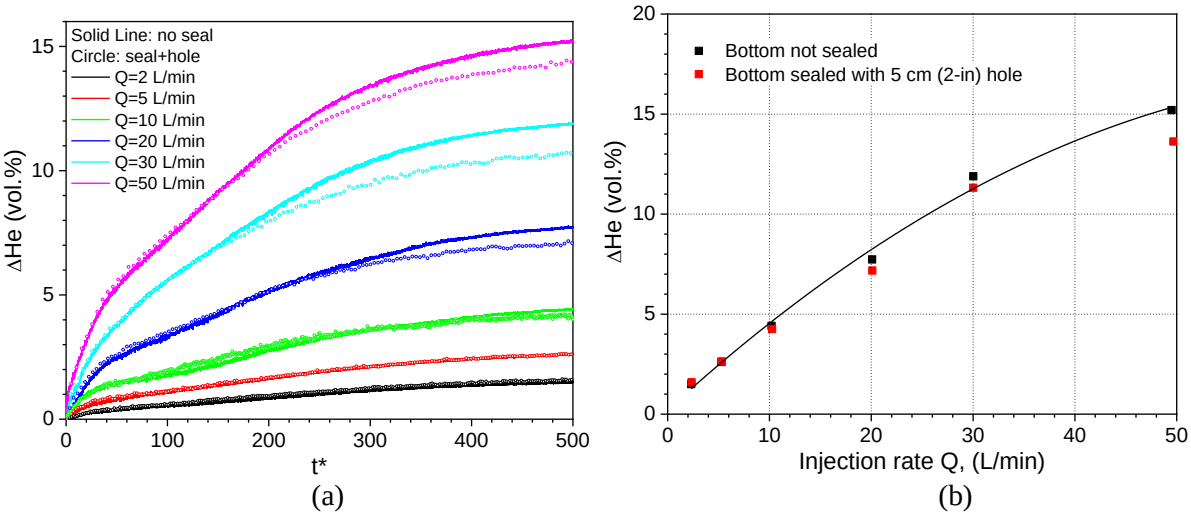

Figure 5. (a) Normalized time transient of vertical helium concentration difference, *ΔHe*, and (b) vertical helium concentration difference at t* = 500

3.4 Helium Concentration Profile

Baines & Turner [1] provided analytical expressions for the filling front downward velocity and the asymptotic state vertical profile when the time approaches infinity, that is, when the filling front arrives at the floor. Worster & Huppert [2] derived an approximate analytical solution for the time-dependent vertical profile when the filling front moves downwards. Worster & Huppert's solution is close to Baines & Turner's solution in the limit of time approaching infinity. Fig. 6 compares the predictions calculated using Worster & Huppert's model with the Configuration 1 measured vertical helium concentration profile at t* = 10–100 for the tests with helium injections of 2, 5, 10, and 50 SLPM. The air entrainment coefficient that appears in the normalization scheme of Worster & Huppert's model was fixed at 0.1.

For the 2 and 5 SLPM test (Figs. 6a and 6b), the measured helium concentration decreases more or less linearly between a height of 1 and 2.5 m at $t^* \leq 20$. After t* = 20, a relatively well-mixed layer is formed above a height of 1.75 m and the decrease in the helium concentration below 1.75 m follows a more or less linear trend. Cariteau et al. [4] showed that, for a flow rate between 1 and 5 SLPM, the helium profile is in the stratified regime, where there is no homogeneous layer thicker than 10% of the height and the helium concentration decreases nearly linearly from the ceiling. Their finding is similar to our results in the early transient. Our measurements are greatly over-predicted at any t* by Worster & Huppert's model even though the time for helium to reach the ceiling is subtracted. Cariteau et al. [4] and Cariteau & Tkaschenko [5] stated that the air entrainment coefficient applied in Worster & Huppert's model had to be adjusted to between 0.06 and 0.08 to match their data, but this adjustment did not improve the agreement for the current study.

For the flow rates of 10 and 50 SLPM (Figs. 6c and 6d), the helium profiles always consist of a homogenous layer above a height of 1.7 m, followed by a gradually decreasing profile. They are similar to the results shown in Cariteau et al. [4] for flow rates greater than 5 SLPM. With an increase in the injection rate, the initial gas velocity will be increased. The flow at the ceiling of the enclosure will also be higher, such that the local mixing can be enhanced, allowing development of a homogeneous layer. The model predictions are in very good agreement with the measurements up to t* = 80. After t* = 80, the measurements are always over-predicted, suggesting that the filling front should have arrived at the floor, where Worster & Huppert's model is no longer valid. Further, leakage becomes significant at larger t*, and the agreement is therefore expected to be poor.

Fig. 7 compares the predictions using Baines & Turner's model with the measured vertical helium concentration at t* = 120 for the tests with Configuration 1. The entrainment coefficient is also fixed at 0.1. The predictions are in good agreement with the measurements for all the tests except for a small deviation for the 30 SLPM test. In the experiment, the decrease in helium concentration below 0.75 m becomes sharp at higher flow rate, which is not reflected in the model. This must be attributed to the effect of air ingress from the bottom and side of the enclosure, which was not considered in the model.

The measured vertical helium profiles at t* = 500 for all the tests are shown in Fig. 8. As already observed in Figs. 4c and 4d, the helium concentration is nearly fully mixed above a height of 1 m at steady state and the concentration decreases to zero sharply below 1 m (Fig. 8a). The concentration difference becomes larger at a higher flow rate. As demonstrated in Fig. 8b, normalizing the helium concentration profile by its average concentration (listed in Table 3) led to superposition of the different profiles, indicating that the steady-state results are self-similar.

Table 3. Average helium concentration at t* = 500

Config.	1 - no seal on floor						2 - seal + 5 cm (2 in) hole in floor					
Q (SLPM)	2.3	5.3	10.2	20.1	30.0	49.5	2.3	5.3	10.3	20.1	30.0	49.6
<He> (%)	3.1	5.0	7.4	10.9	13.7	17.7	3.2	5.1	7.7	11.2	13.8	19.0

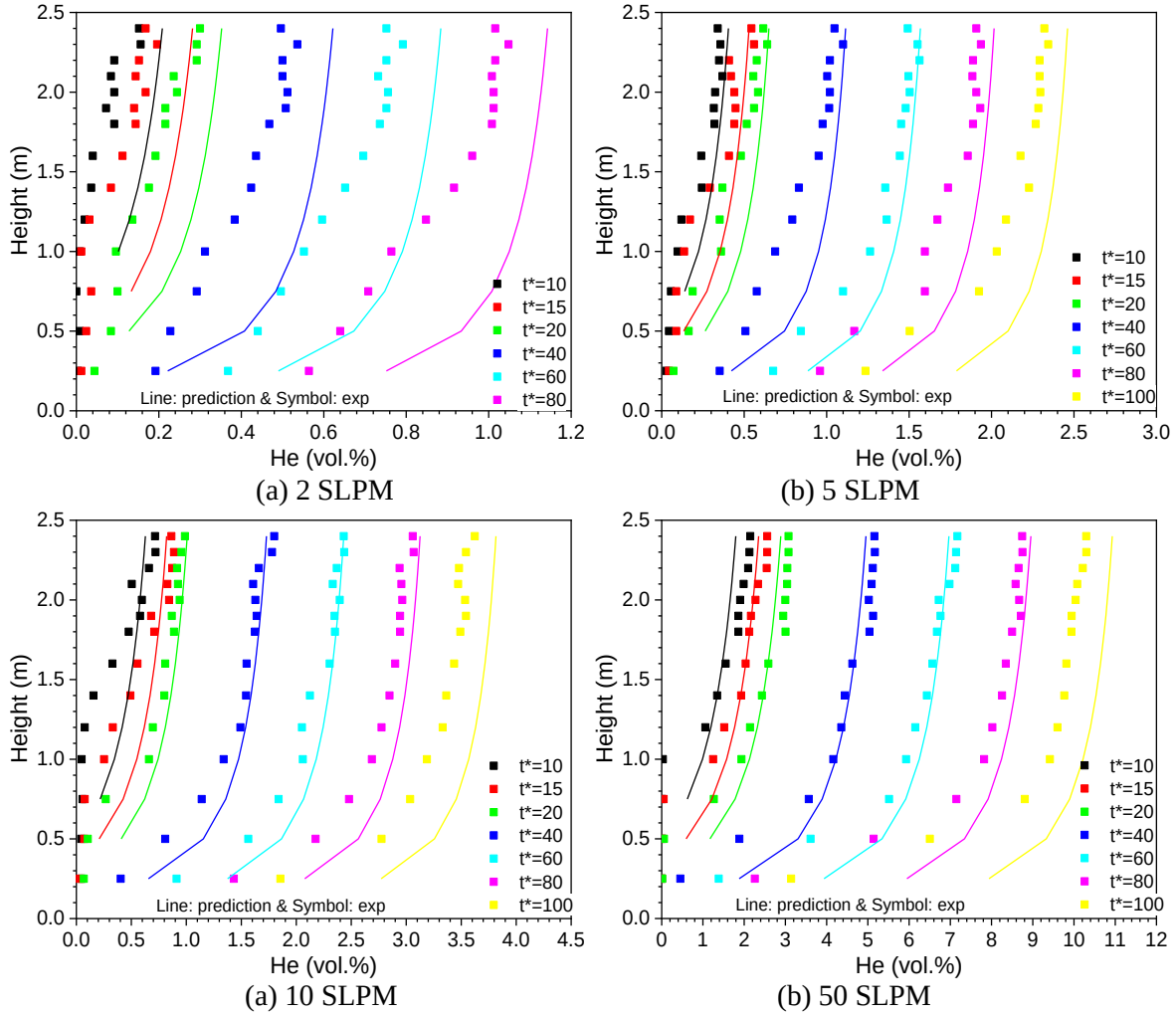

Figure 6. Comparison of measured and calculated (with Worster & Huppert's model [2]) vertical helium concentration profiles during propagation of initial front for 2, 5, 10, and 50 SLPM tests (Configuration 1)

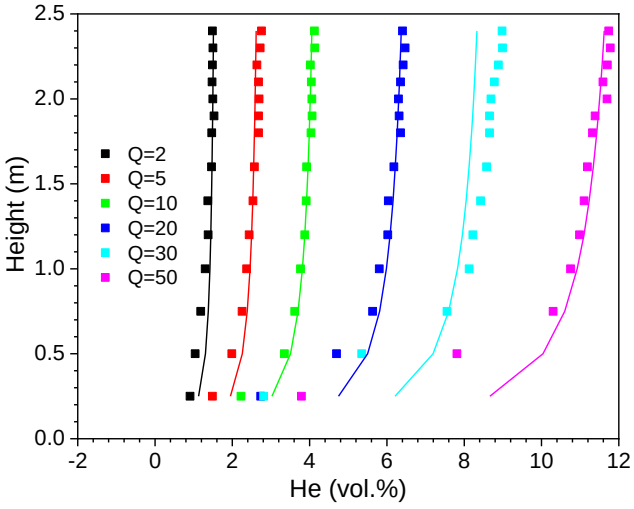

Figure 7. Comparison of vertical helium concentration profiles at t* = 120 for 2–50 SLPM tests against Baines & Turner's solution [12]

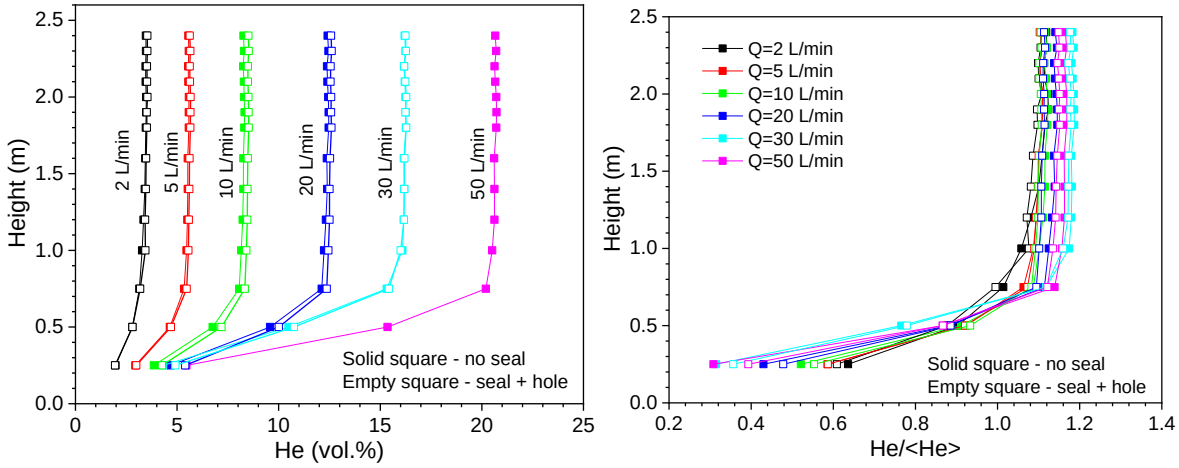

Figure 8. Vertical helium profiles at t* = 500 for (a) volume concentration, and (b) normalized with average volume concentration

3.5 Inflow Velocity

The sensitivity of the opening location, in Configuration 2, was studied by relocating the 2 in (5 cm) hole away from the helium sensors and performing additional tests with injection rates of 2, 20, and 50 SLPM. The helium distribution is identical for the same injection rate shown in Figs. 5 and 8, suggesting that the location of air ingress had no influence on helium distribution. The inflow velocity at the opening was measured in these tests and is plotted against the normalized time in Fig. 9. The signals are smoothed using a 100 Hz low–pass filter. For the 2 SLPM injection rate, air enters the enclosure at an average speed close to 0.39 m/s (7.9×10^{-4} m^3/s or 47 SLPM), and increases to approximately 0.98 m/s (2.0×10^{-3} m^3/s or 119 SLPM) for the 20 SLPM test and 1.14 m/s (2.3×10^{-3} m^3/s or 139 SLPM) for the 50 SLPM test. The inflow rates are of the same magnitude as the leak rate discussed in Section 3.1.

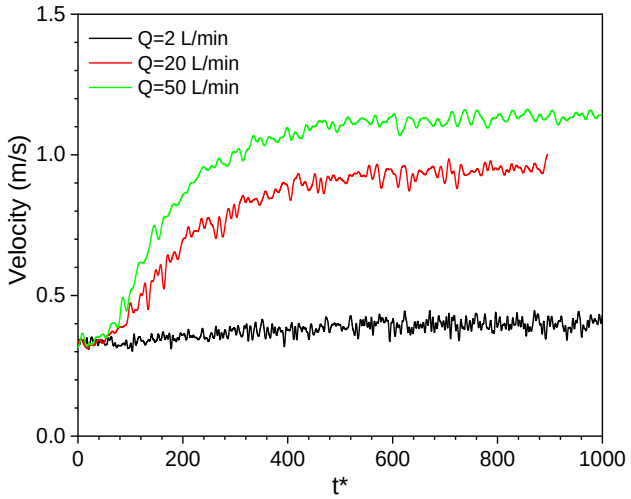

Figure 9. Transient of inflow velocity through opening in Configuration 2 for tests with 2, 20, and 50 SLPM

4.0 CONCLUSIONS

An experimental study was performed to examine helium dispersion behaviour in a 16.6 m^3 semi-confined enclosure. The release was a vertical helium jet from a nozzle located near the floor at a flow rate of 2 to 50 L/min. The results are similar for the two test configurations: (1) with distributed leaks along the edges of the floor (well-sealed on other surfaces), and (2) a relatively well-sealed enclosure

with a 5 cm (2 in) opening in the floor. The leakage rate determined using the average helium concentration decay is close to 0.3–0.4 air changes per hour.

Two types of filling regimes are observed during the short-term transient: stratified or stratified with a homogeneous layer, depending on the flow rate (injection Richardson number). In a long-term transient with vertical helium injection from the floor, the helium profile always reaches a steady state with an upper homogenous layer (>1 m height) and a stratified layer below a height of 1 m , suggesting that the entering fresh air due to leakage moves downward and dilutes the mixture near the floor. The steady-state vertical helium profile is approximately self-similar when the helium concentration is normalized by its volume-averaged concentration.

For a flow rate greater than 5 SLPM, the vertical helium profile matches well with the prediction using Worster & Huppert's model [2] when the filling front moves downwards. When the filling front reaches the floor, good agreement is also found between the measured vertical helium profile and the prediction using Baines & Turner's model.

ACKNOWLEDGEMENT

The authors gratefully acknowledge the financial support from Atomic Energy of Canada Limited, under the auspices of the Federal Nuclear Science and Technology Program.

REFERENCE

1. Baines, W.D. and Turner, J.S., Turbulent Buoyant Convection from a Source in a Confined Region, *J Fluid Mech*, **37**, Part 1, 1969, pp. 51–80.
2. Worster, M.G. and Huppert, H.E., Time-Dependent Density Profiles in a Filling Box, *J Fluid Mech*, **132**, 1983, pp. 457–466.
3. Bolster, D.T. and Linden, P.F., Containments in Ventilated Filling Boxes, *J Fluid Mech*, **591**, 2007, pp. 97–116.
4. Cariteau, B., Brinster, J., and Tkatschenko, I., Experiments on the Distribution of Concentration due to Buoyant Gas Low Flow Rate Release in an Enclosure, *Int J Hydrog Energy*, **36**, 2011, pp. 2505-2512.
5. Cariteau, B. and Tkatschenko, I., Experimental Study of the Concentration Build-Up Regimes in an Enclosure without Ventilation, *Int J Hydrog Energy*, **37**, 2012, pp. 17400–17408.
6. Gupta, S., Brinster, J., Studer, E., and Tkatschenko, I., Hydrogen Related Risks within a Private Garage: Concentration Measurements in a Realistic Full Scale Experimental Facility, *Int J Hydrog Energy*, **34**, 2009, 5902–5911.
7. Houssin-Agbomson, D., Letellier, J-Y., Renault, P., and Jallais, S., An Experimental Study Dedicated to Wind Influence on Helium Build-Up and Concentration Distribution Inside a 1-M^3 Semi-confined Enclosure Considering Hydrogen Energy Applications Conditions of Use, International Conference on Hydrogen Safety, 2015 October 19–21, Yokohama, Japan.
8. Bernard-Michel, G. and Houssin-Agbomson, D., Comparison of Helium and Hydrogen Releases in 1 m^3 and 2 m^3 Two Vents Enclosures: Concentration Measurements at Different Flow Rates and for Two Diameters of Injection Nozzle, International Conference on Hydrogen Safety, 2017 September 11–13, Hamburg, Germany.
9. Voelsing, K., GOTHIC - Thermal Hydraulic Analysis Package Technical Manual Version 8.2 (QA), Electric Power Research Institute Inc., 2016 October.
10. Liang, Z. and Chin, Y-S., Simulation of Buoyancy Induced Gas Mixing Tests Performed in a Large Scale Containment Facility Using GOTHIC Code, Proceedings of 19th Pacific Basin Nuclear Conference (PBNC), 2014 August 24–28, Vancouver, BC, Canada.
11. Xensor Integration, Installation of the CAN Bus Network for the XEN-5320-CAN, 2018 August 28.
12. Papanicolaou, P.N. and List, E.J., Investigation of Round Vertical Turbulent Buoyant Jets, *J Fluid Mech*, **195,** 1988, pp. 341–391.
13. Cleaver, R.P., Marshall, M.R., and Linden, P.F., The Build-Up of Concentration within a Single Enclosed Volume Following a Release of Natural Gas, *J Hazard Mater*, **36**, 1994, pp. 209–226.